

# The LINC-NIRVANA Cryogenic Interferometric Camera

P.Bizenberger<sup>\*a</sup>, D.Andersen<sup>a</sup>, H.Baumeister<sup>a</sup>, U.Beckmann<sup>b</sup>, E.Diolaiti<sup>c</sup>, T.Herbst<sup>a</sup>, W.Laun<sup>a</sup>,  
L.Mohr<sup>a</sup>, V.Naranjo<sup>a</sup>, C.Straubmeier<sup>d</sup>

<sup>a</sup>Max Planck Institut für Astronomie, Königstuhl 17, 69117 Heidelberg, Germany

<sup>b</sup>Max Planck Institut für Radioastronomie Bonn, Auf dem Hügel 69, 53121 Bonn, Germany

<sup>c</sup>Osservatorio Astrofisico di Arcetri, L.goE. Fermi 5, 50125 Firenze, Italy

<sup>d</sup>Physikalisches Institut Universität Köln, Zùlpicher Str. 77, 50937 Köln, Germany

## ABSTRACT

The LINC-NIRVANA instrument is a 1-2.5 micron Fizeau interferometric imager, which combines the light of the two 8.4 m mirrors of the Large Binocular Telescope on Mt. Graham in Arizona. The cryogenic camera forms the heart of the science channel of this instrument, delivering a 1 arcmin diameter field of view with 5 mas spatial resolution. The center 10x10 arcseconds, initially limited by the size of the 2048x2048 Hawaii-2 detector, are used for science observations. For simplicity, the camera has a fixed, f/32 optical path of the combined beams, leading to wavelength-dependent sampling. We describe the main components of the camera, as well as present the calculations of interferometric performance and the required opto-mechanical tolerances. We demonstrate that specially designed components can reach these specifications.

**Keywords:** interferometric camera, cryogenic interferometer, LBT instrumentation, Fizeau

## 1. INTRODUCTION

The LINC-NIRVANA cryogenic interferometric camera actually combines and interferes the light from the two 8.4 m mirrors<sup>1</sup> of the LBT and which has been collimated by the warm optics<sup>2</sup> located behind the F/15 telescope focus. The optical interface to the cryogenic camera is the double pupil of the LBT re-imaged by the collimators located just inside the cryostat thereby providing a cold pupil stop. The ratio of diameter and separation of the cold pupils are a scaled down version of the entrance pupils of the two telescopes to fulfill the sine condition<sup>3</sup>. These two pupils are focused with a common reflective optics to a 1 arcmin diameter image plane. This large field of view is used for fringe tracking. The center 10 arcsec x 10 arcsec are reflected off via various, selectable dichroic mirrors to a HAWAII2 detector. This detector covers the wavelength range from 1 to 2.4  $\mu\text{m}$ , from J to K band respectively. The fringe tracking detector (HAWAII1) is sensitive to the same wavelength range i.e. science observations will be taken in one band and fringe tracking will be done in one of the other bands.

The requirements for optical quality and mechanical accuracy are very high. They are driven by two critical issues. A high fringe contrast in the interferometric focus is needed to achieve the lateral resolution of the 23 m baseline. Therefore the optical quality must be diffraction limited for a 23 m class instrument with the required large field of view for fringe tracking. The mechanical tolerances are very tight, particularly flexure, to avoid de-correlation of the two arms. Simulations demonstrate that mechanical accuracy and aligning must be in the range of a few arcseconds. Therefore a lot of effort was taken for the design and for prototypes to demonstrate the feasibility of the cryogenic units.

## 2. INSTRUMENT OVERVIEW

The whole interferometric camera is mounted inside a large cryostat. All components are cooled with a closed loop system<sup>4</sup>. Because of the already mentioned high mechanical requirements the heat exchanger is designed as a ridged structure where all the internal components are mounted to. The heat exchanger is cylindrically shaped, so all thermal expansions will be radial and can be easily calculated. In the following sketch all main units are labeled. Units are sub-systems as e.g. the detector rotation stage, with several mechanical and electrical functions. The warm optics, the AO sensors and the deformable mirrors are indicated. The LINC-NIRVANA instrument uses two off center foci of the LBT i.e. the beams from the left and right telescope are tilted by 18° to the center line.

\* [biz@mpia.de](mailto:biz@mpia.de) phone (+49) 6221 528311

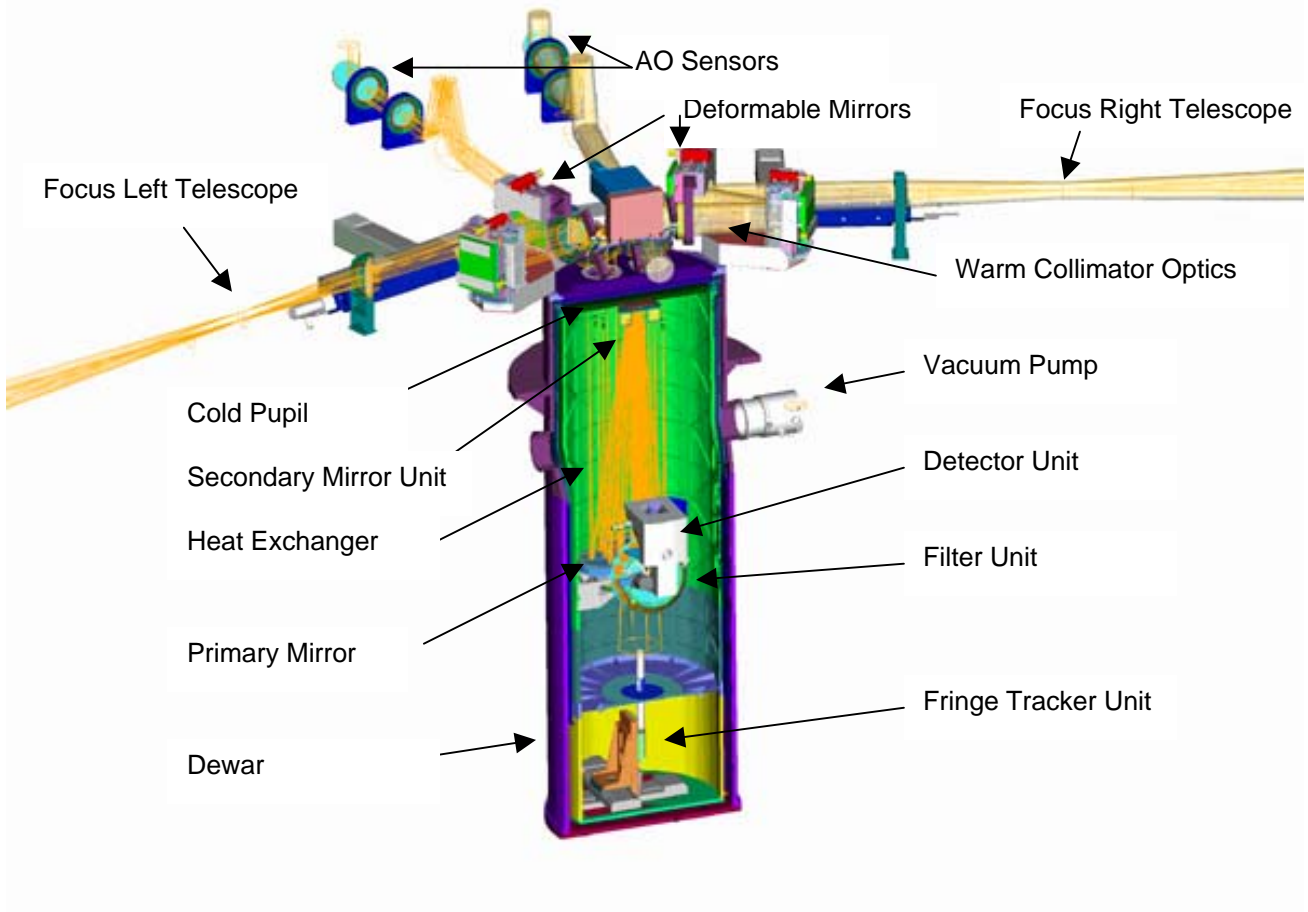


**Figure 1:** Layout of the LINC-NIRVANA cryostat.

### 3. OPTICS

#### 3.1 Sampling & F-ratio requirements

A requirement for image reconstruction is the sampling of 2 pixels per  $\lambda/B$  at the shortest wavelength, where  $B$  is the longest baseline of the LBT configuration (Figure2). For the selected HAWAII2 detector with  $18\mu\text{m}$  pixel pitch a final F/88 beam for the individual telescope and F/32 for the combined focus is required (Figure3). For the design the equivalent paraxial focal length is used because of the non symmetric pupil configuration.

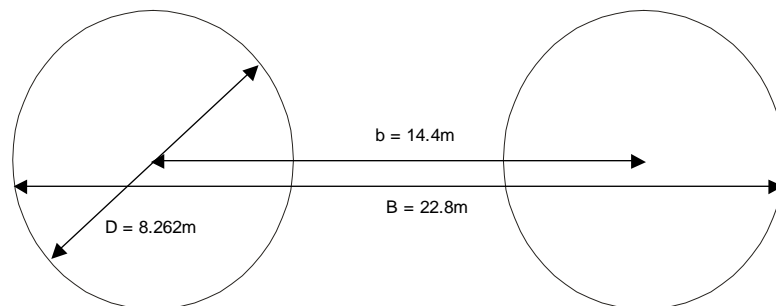


**Figure 2:** LBT dimensions and baselines

Band	Wavelength $\mu\text{m}$	Detector $\mu\text{m}/\text{pixel}$	Sampling for $\lambda/B$	$\lambda/D$				pixel scale mas/pixel	$F\#$ required	$F\#$ single arm	for $F\#$ single arm		for $F\#$ selected		
				FWHM @8.4m mas	$\lambda/B$ FWHM @22.8m mas	$\lambda/B$ FWHM @22.8m $\mu\text{m}$	$\lambda/b$ 1.Min. mas				FOV for 2k array arcsec	Corner for 2k array degrees	$F\#$ selected	FOV for 2k array arcsec	Corner for 2k array degrees
J	1,00	18	1,8	24,6	9,0	5,4	14,3	5,11	31,9	87,9	10,5	0,00205613	88	10,5	0,00205404
	1,13	18	2,0	28,2	10,2	6,1	16,2	5,11	31,9	87,9	10,5	0,00205613			
	1,25	18	2,2	31,2	11,3	6,8	17,9	5,11	31,9	87,9	10,5	0,00205613			
	1,37	18	2,4												
H	1,50	18	2,7	37,4	13,6	8,2	21,5	5,11	31,9	87,9	10,5	0,00205613	88	10,5	0,00205404
	1,65	18	2,9	41,2	14,9	9,0	23,6	5,11	31,9	87,9	10,5	0,00205613			
	1,80	18	3,2												
K	1,90	18	3,4	47,4	17,2	10,3	27,2	5,11	31,9	87,9	10,5	0,00205613	88	10,5	0,00205404
	2,15	18	3,8	53,7	19,5	11,7	30,8	5,11	31,9	87,9	10,5	0,00205613			
	2,40	18	4,2												

**Figure 3:** Sampling and required F/# versus wavelengths

Further on, simulations<sup>5</sup> show that the foci of the two telescopes must be within  $0.5 R_{\text{Airy}}$  of an individual telescope in order to archive the required fringe contrast of  $> 90\%$ . A larger separation of the two PSFs would decrease very fast the fringe contrast. This requirement is more or less equivalent to keep the two PSFs within a 23m Airy diameter which is used for the optical design merit function.

### 3.2 Design

The actual design of the combining optics is done without the telescopes and the warm collimating optics. Since the optical quality of the collimator design is superb, this can be assumed as perfect and will be used only for verification. The optics are designed as a sort of Cassegrain telescope which is used only partially at an off center area, even though the telescope design is on axis. Figure 4 illustrates the layout, the two arrows indicate the two incoming, collimated beams. The two collimated beams enter the cryostat through two dewar windows. The primary mirror of the Cassegrain telescope is only partially illuminated. This design was selected to maximize the field of view for fringe tracking. The field of view with sufficient optical quality for fringe tracking is 1 arcmin diameter, but the image plane is curved. This must be leveled out by the fringe tracker, which moves across the field in x, y and z direction. The science field is split off by a dichroic mirror and is flat. The bending of the window due to vacuum and the slightly curved detector is taken into account in the design.

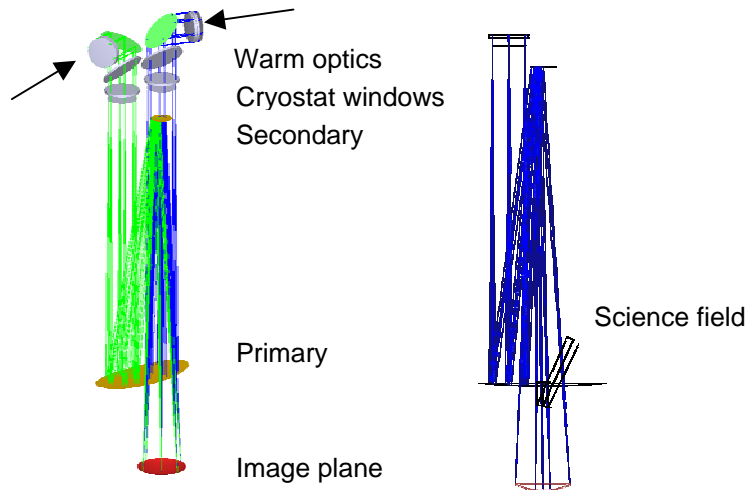


**Figure 4:** Layout of the IR optics. Left: The warm optics, dichroics and windows are indicated. Right: Schematic of the Cassegrain design with the folded science arm. The second interferometric channel is located behind the paper plane.

The achieved optical quality for fringe tracking is sufficient (Figure 5) even at the edge of the 1 arcmin diameter field of view. In the following OPD diagrams, the y direction of the fan is shown only, because the x direction is blanked off by the user defined aperture. An elliptical aperture covering the real two apertures approximates the illumination and verifies the OPD in x direction but is not shown here in this paper. Simulations show that  $\lambda/2$  is borderline for fringe tracking but still possible, as can be seen in Figure 6 . The fringe contrast is low, but the fringes are still well separated.

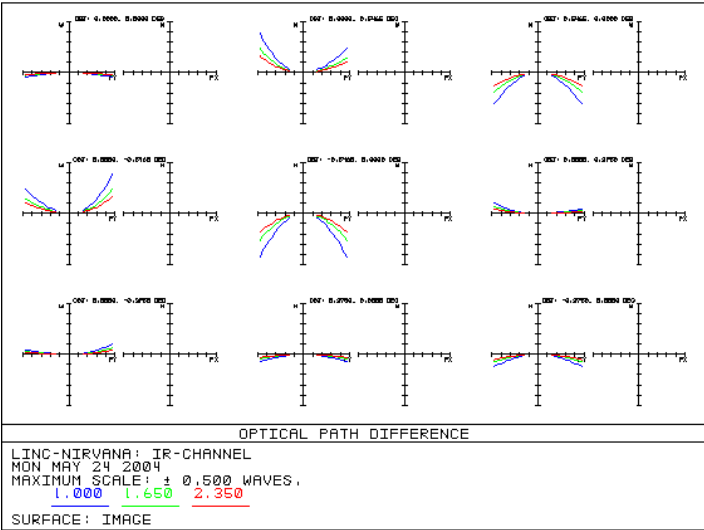


**Figure 5:** Optical path difference for the fringe tracking field of view. Field positions are one center, 4 times edge and 4 times intermediate fields.

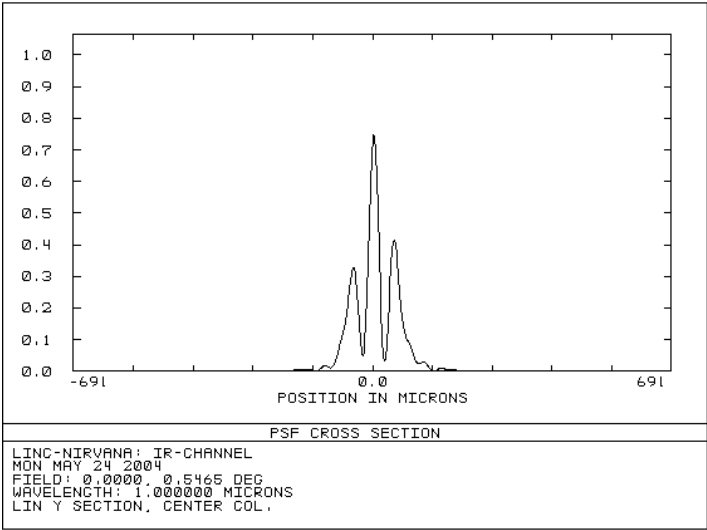


**Figure 6:** PSF cross section for field position at the edge of the 1 arcmin diameter field of view.

The optical quality for the center science field is sufficient, even for a flat image plane. The field dependant defocus can be minimized by shifting the detector 0.5 mm towards the secondary. The remaining aberrations are less than  $\lambda/10$  at  $1\mu\text{m}$ .

The de-correlation of the left and right channel is less than a 23 m PSF as can be seen in Figure 9. This fulfills the already mentioned fringe contrast requirement.

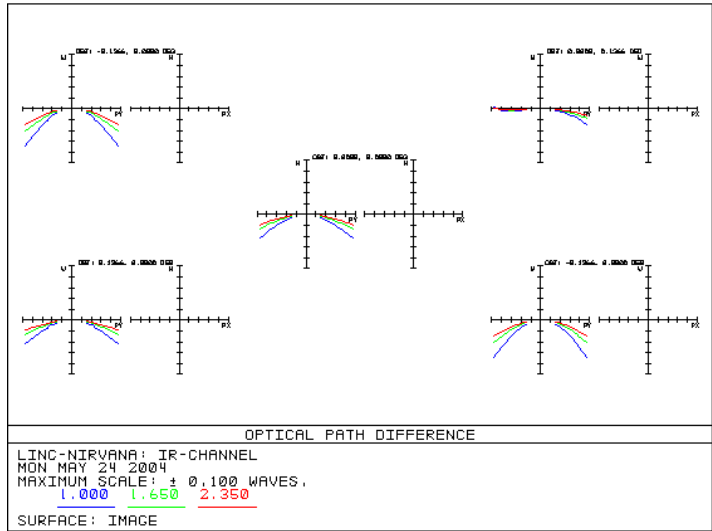


**Figure 7:** Optical path difference for the science field of view.

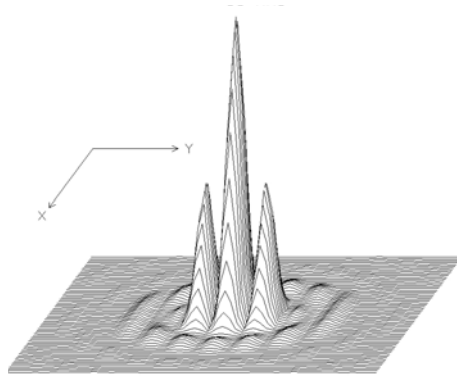


**Figure 8:** Calculated PSF at the science detector.

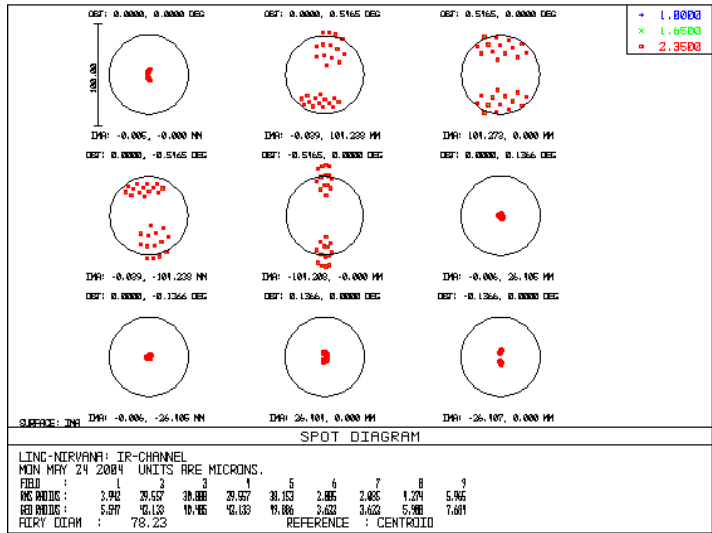


**Figure 9:** Spot Diagram of fringe tracker and science field. The separation of the left and right channel are present, but less than one 23 m PSF at the edge of the fringe tracker field. Circles represent a 23 m Airy ring at 1  $\mu$ m.

### 3.3 Verification

To verify the optical design, the common IR optics are added to the telescope and collimator design. This is presently only done for the 8.4 m configuration. The left and right channel are handled in two Zemax configurations. Here, no interferometric analysis is possible, but the optical performance could be verified. No additional aberrations are introduced as assumed. This also proves the assumption for this simple approach of interferometric optical design.

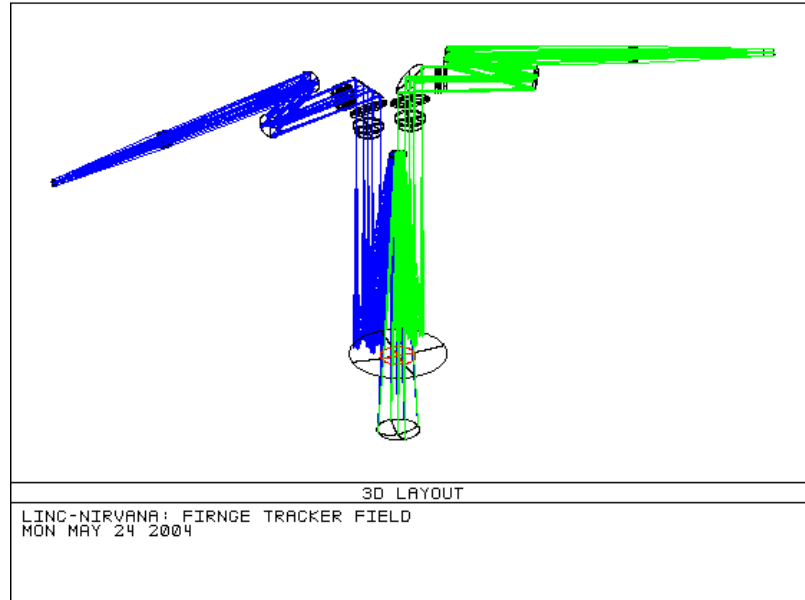


**Figure 10:** Optical design including telescopes, warm collimators, dichroic mirrors and vacuum windows.

## 4. CRYO-MECHANICS

### 4.1 Detector rotation unit

LINC-NIRVANA is mounted on the Nasmyth focus of LBT. There is, of course, no image de-rotator applied, i.e. the sky is rotating on the final image plane and the pupil is fixed. In order to follow the stars, the detector must be rotated. Since the pupil is fixed, rotating the detector means that the fringes of the PSF now rotate with respect to the detector pixels. Simulations<sup>6</sup> demonstrate that an angle of rotation limited to 30° delivers PSFs without a significant loss of fringe contrast. The extracted tolerances require a 15 arcsec resolution for the rotation. This spec is far tighter than the given specs for commercial gears. However, we tested a harmonic drive modified for cryogenic operations that actually meets the requirements on absolute positioning and repeatability. The tests<sup>7</sup> are done with an auto collimation telescope and/or a laser-CCD setup. Both setups are suitable for making measurements in ambient conditions or cryogenic conditions.

Conventional amplifiers (PWM) for stepper motors would add noise to the detector if used during readout as it is the case for a detector rotator. Therefore an analog amplifier is used. The sinusoidal current does not introduce any measurable noise even if the motor is used very close to the detector. (Figure 12)

Simulations<sup>6</sup> also demonstrate that the axis of rotation must be co-aligned with the optical axis within one pixel to avoid fringe smearing. Therefore the detector rotation unit must be aligned to less than one pixel, i.e. less than 18 $\mu$ m, in cryogenic environment. This tolerance is also valid for any flexure during operation where the cryostat is tilted up to 60° when pointing the telescope to the limit of interferometric observing 60° off zenith maximum. To align the detector to the optical axis, two cryogenic actuators<sup>7</sup> are added.

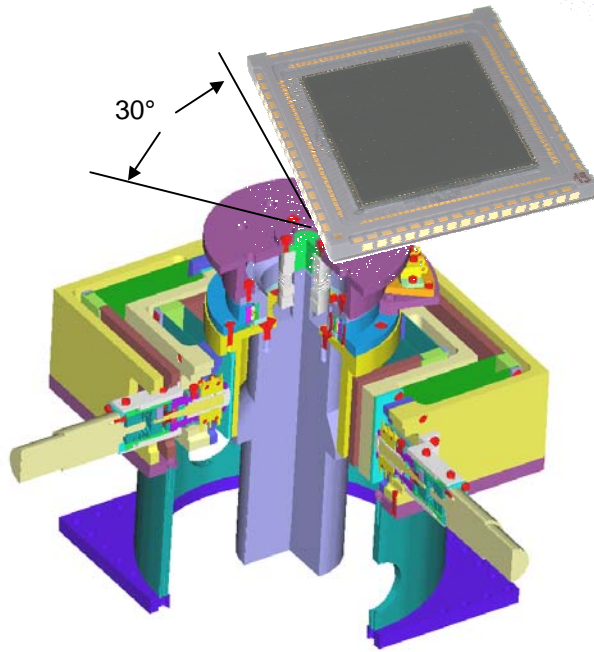


**Figure 11:** Cryogenic detector rotation unit. Angle of rotation is limited to 30°.

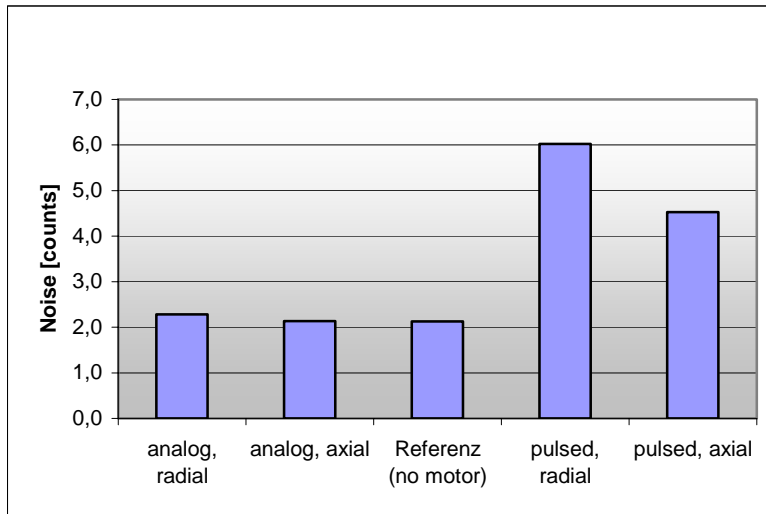


**Figure 12:** Added noise through analog and pulsed stepper motor amplifier for various mounting orientations.

#### 4.2 Dichroic and filter wheel unit

The fringe tracking field and the science field are separated by a dichroic mirror. Since fringe tracking and science detector are sensitive in the same wavelength range, various beam splitters are required to define observing and tracking wavelengths e.g. observing in K band and tracking in H band. This set of mirrors is mounted in a wheel directly driven by a Phytron motor. Tolerances for the angle of reflection are already mentioned in the previous section. In order to keep the optical axis and the axis of rotation within one pixel, the tilt of the wheel must be less than 10 arcsec. Therefore special cryogenic ball bearings from ADR with very small clearance are used. They are mounted in an identical steel

alloy to avoid thermal stress. Because of the steel mounting, an additional thermal connection is required. To verify the performance of the design, a prototype (Figure 12) was built. Final test results are not available yet, but first tests are promising in terms of cool down and moving precision.

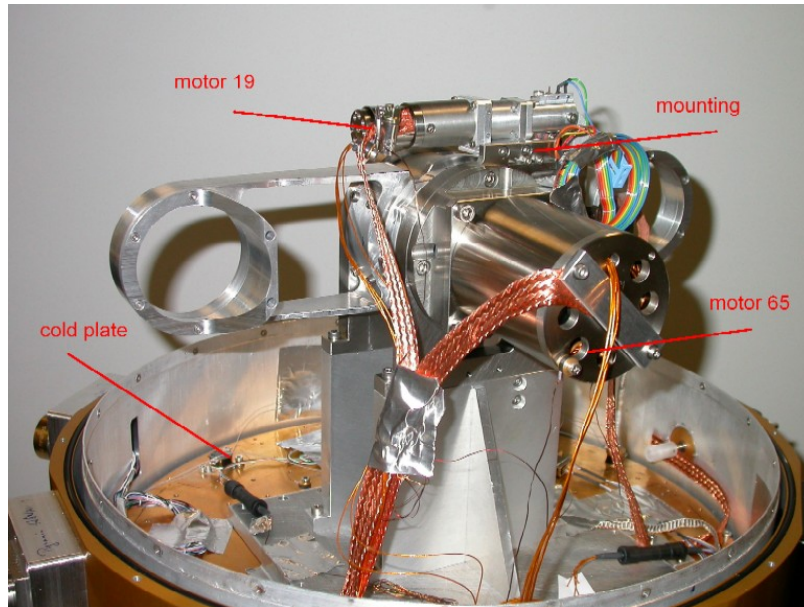


**Figure 13:** Prototype of the dichroic wheel unit. Phytron motors are used for driving and thermal connection.

#### 4.3 Secondary mirror unit

The secondary mirror is used to remotely adjust the cold optics. Tip-tilt and focus can compensate for manufacturing and assembly tolerances. If necessary, it can be used to compensate flexure of the common path, i.e. of the cryostat. These functions are done with a three axis mount, driven with cryogenic actuators<sup>7</sup>. This design is already used for aligning CCD detectors and has proven feasibility.

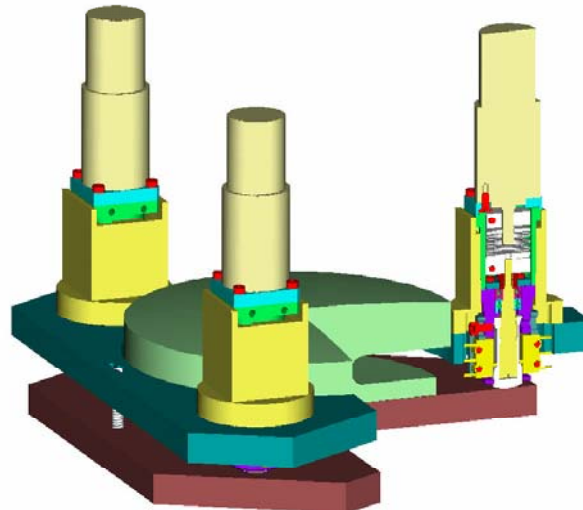


**Figure 14:** Design of the secondary mirror unit.

#### 4.4 Fringe tracking unit

The fringe tracking unit is listed here only for completeness. A detailed description is given by Straubmeier et al.<sup>5</sup>

#### 4.5 Cryostat and Vacuum System

The cryostat system consists of three major components:

- Cryostat and vacuum equipment
- Heat exchanger
- Cooling system

The main requirement for the cryostat is stiffness. But it can be supported by the mounting structure of the whole LINC-NIRVANA instrument, so bending is a minor problem. The heat exchanger acts as support structure for all internal optics and cryogenic units. Cylindrically shaped with precise processing of reference planes, it is the reference for the assembly of the IR channel. The cooling is done with a closed loop system using a flow of Helium gas. All system components are described in detail by Laun et al.<sup>4</sup>.

## 5. SCIENCE DETECTOR & READOUT SYSTEM

### 5.1 Detector

The science detector is a 2048x2048 HgCdTe HAWAII2 device from Rockwell Scientific. The selected PACE type is sensitive from  $\sim 1 \mu\text{m}$  to  $\sim 2.5 \mu\text{m}$  and covers J, H and K band for science observations. It will be operated as in the LUCIFER instrument<sup>8</sup> since the requirements in terms of read noise, dark current and typical integration time are very similar.

### 5.2 Readout System

The detector readout system consists of three major components:

- Readout electronics
- Software on UNIX or LINUX platform
- Patterns controlling the detector timing for the various readout modes

The readout electronics are built at MPIA and are used already in several instruments as in Omega2000<sup>9</sup>, MIDI and LUCIFER<sup>8</sup>. The readout electronics are connected via fiber link to the detector control computer. There, the detector control software GEIRS<sup>10</sup> running under SOLARIS or LINUX is pre-processing the data and controlling the detector. Data pipelines and image reconstruction software can be connected to this software as done for Omega2000. The detector timing patterns are a set of several ASCII files defining the readout modes, the integration time, idle loops, cycle repeats etc. These files are updated online by GEIRS software and sent to the readout electronics, e.g. if the readout mode is switched, integration time is changed or any other observing parameters are modified. This modular system is very flexible, any changes to the detector patterns can be done on a short time scale, i.e. editing an ASCII file.

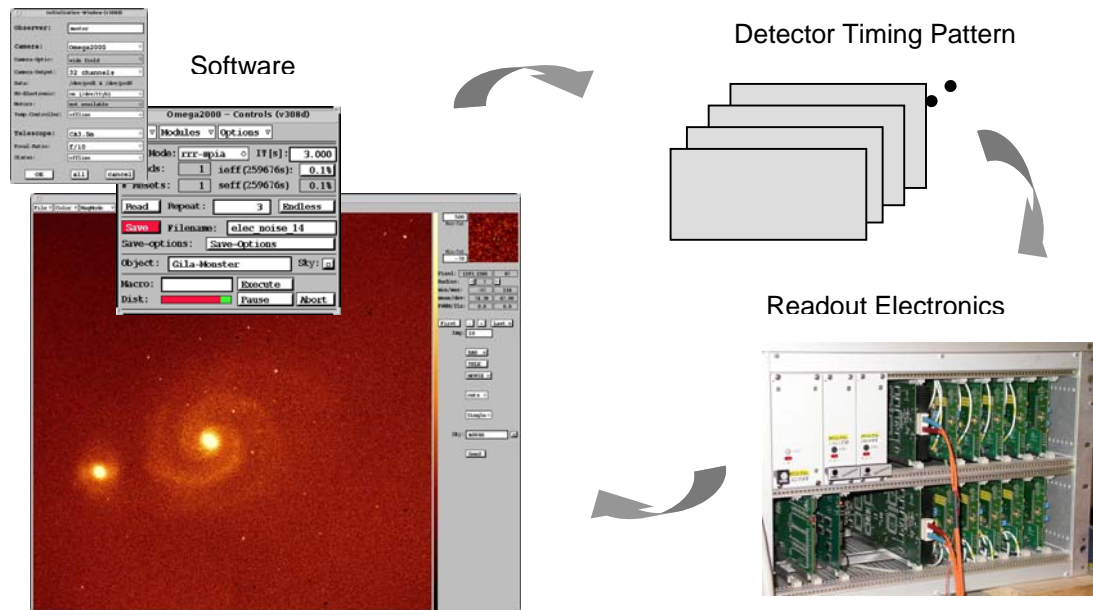


**Figure 15:** Arrangement of the readout system, consisting of three major components.

## REFERENCES

1. J.M. Hill, P. Salinari, "The large Binocular Telescope Project", SPIE 4004-07, 2000
2. W. Xu et al., "LINC-NIRVANA warm optics: combining the needs of the interferometer and MCAO System", SPIE conference Glasgow 2004, 5492-97
3. W.A. Traub, "Combining beams from separated telescopes", Applied Optics, Vol. 25, No. 4, 15.Feb.1986
4. W. Laun et al., "Cooling of ground based telescope instrumentation, the LINC-NIRVANA cryostat", SPIE conference Glasgow 2004, 5492-125
5. C. Straubmeier et al., "A fringe and flexure tracking system for LINC-NIRVANA: basic design and principle of operation", SPIE conference Glasgow 2004, 5491-171
6. D. Andersen et al., "LINC-NIRVANA testbed Fizeau interferometer", SPIE conference Glasgow 2004, 5491-207
7. Rohloff et al, "Cryogenic actuators in ground-based instrumentation", SPIE conference Glasgow 2004, 5495-87
8. S. Ligori et al., "The MPIA detector system for the LBT instruments LUCIFER and LINC-NIRVANA", SPIE conference Glasgow 2004, 5499-33
9. Z. Kovacs et al., "Characterization, testing, and operation of the OMEGA2000 NIR wide-field camera", SPIE conference Glasgow 2004, 5499-48
10. C.A.L. Bailer-Jones, P. Bizenberger, C. Storz, "Achieving a wide field near infrared camera for the Calar Alto 3.5m telescope", SPIE Vol.4008, March 2000